EARTHQUAKE ENGINEERING AND STRUCTURAL DYNAMICS, VOL. 25, 965–985 (1996)

BUILDING DUCTILITY DEMAND: INTERPLATE VERSUS INTRAPLATE EARTHQUAKES

NELSON LAM*, JOHN WILSON† AND GRAHAM HUTCHINSON‡

Department of Civil and Environmental Engineering, The University of Melbourne, Parkville 3052, Victoria, Australia

SUMMARY

The inelastic seismic response behaviour for a range of simplified single-degree-of-freedom models has been analysed using 180 random phase angle synthetic accelerograms with different frequency contents and different durations and 105 real accelerograms collected from different regions worldwide. Results from the analyses have identified that the frequency content of the excitation can greatly influence the ductility demand ratio due to inelastic amplification effects. Consequently, results derived from intraplate earthquake records (typically of higher frequency content) were generally different to those from interplate records. However, the commonly used El Centro accelerogram has significantly lower ductility demand in the low period range than the average of records with similar elastic response spectral shape. Apart from this, there was little evidence to suggest any inherent differences in the inelastic response behaviour of buildings from intraplate and interplate earthquakes which possessed similar frequency content. Thus, the average ductility demand ratios from future earthquakes in an area can be predicted by interpolation of the results presented in this paper assuming the elastic response spectrum has been defined. Ductility demand ratios derived from the synthetic accelerograms and the real accelerograms with similar frequency content have been shown to be consistent. However, results from synthetic records derived for the idealised code design spectra (such as the Uniform Building Code and the Australian Standard AS1170.4) indicate a significantly higher ductility demand in the long period range.

KEY WORDS: ductility; earthquakes; seismic; intraplate; building; inelastic

1. INTRODUCTION

Most earthquakes around the world occur on well defined tectonic plate boundaries, and are known as inter-plate earthquakes. Earthquakes which occur within a tectonic plate are called intraplate. These occur less frequently, and are spread across the whole of the plate rather than being confined to the boundaries. In an intraplate area, such as Australia, it is impossible to predict the location or the likely time of an earthquake event. However, it is now widely accepted that the risk of intraplate earthquakes and their potential for damage in populated areas can no longer be ignored. Major intraplate earthquakes have occured recently in Egypt, Iran, India and China causing significant damage and loss of life. An earthquake of only moderate magnitude (5·6 on the Richter scale) in Newcastle, Australia caused considerable damage and it was only through good fortune that the casualty list was not worse than the 13 killed and 120 injured.[1–3]

There has been growing concern over intraplate seismic risks for the last decade. This has been reflected in recent seismological studies investigating the source and attenuation characteristics of intraplate earthquakes.[4–7] Seismic hazards in a number of low seismicity intraplate areas including eastern North America, Australia, Europe and part of southern China have been evaluated using local instrumented records and qualitative historical records. These studies were concerned mainly with estimating peak accelerations or peak velocities.[4,8–10]

*Research Fellow
†Senior Lecturer
‡Professor of Civil Engineeering and Head of Department

CCC 0098–8847/96/090965–21

Received 29 September 1995
Revised 24 April 1996

In order to predict realistically a building's response to future earthquakes, strong motion accelerograms representative of local seismicity and geology are required. However, for intraplate areas the accelerograms that are available have been predominantly recorded from small events often at large distances. The lack of near field data for moderate to large intraplate earthquakes has meant that in intraplate areas seismic design provisions are often based on codes of practice from regions of high seismic interplate activity such as California.[11–13]

The engineering properties of intraplate earthquakes have been studied by modelling the spectral density of seismic shear waves using a parametric model developed by Hanks and McGuire.[14] A few intraplate elastic response spectra were subsequently derived by stochastic random process theory and by analyses of a number of intraplate ground motion records.[13,15–17] Whilst intraplate earthquake research has been devoted mainly to establishing the frequency content of seismic waves and their elastic amplification in structures, contemporary buildings are normally expected to respond inelastically to severe earthquake excitations. Inelastic designs for seismic effects are based on a load reduction factor which reflects the building's ductility and overstrength. However, recommended modifications to design spectra used in intraplate areas have been largely derived considering elastic response only. Load reduction factors to be used in conjunction with these elastic spectra are usually assumed to be identical to those adopted for inter-plate areas.[11,13]

Conventional aseismic design procedures use elastic analyses to predict structural response. These responses are then modified to account for the inelastic behaviour of the structure. The modification is usually based on either the assumption of equal displacement or equal total energy in the elastic and inelastic systems. These techniques are approximate and have been shown to be not always reliable due to a large scatter in the predicted versus actual responses.[18,19] Whilst it is recognised that this scatter is a problem in interplate areas where many earthquake records exist, in intraplate areas, which have a paucity of data the problem is even further exacerbated.

The load reduction factors which are presented in earthquake loading standards are usually based on the equal displacement concept modified to reflect the performance of different structural systems in past earthquakes.[20] Due to the built-in empiricism in these load reduction factors, it is questionable whether they should be used in an entirely different intraplate environment where the properties of the ground motion and the buildings could be very different.

The objective of this paper is to study the relationship between the ductility demand ratio and the parameters characterising the ground motion properties (i.e. phase angles, duration and frequency content) in both interplate and intraplate areas. An ensemble of 180 synthetic and 105 real accelerograms have been systematically analysed for a wide range of building models to assess their inelastic response behaviour. The accelerograms reflect a range of elastic response spectral shapes to enable the ductility demand to be correlated directly with the ground motion frequency characteristics. Consequently, once the ground motion frequency content has been established for an area, the ductility demand can be readily predicted by interpolation of the results. Results from random phase-angle synthetic records which may not realistically represent the non-stationary characteristics of real earthquake ground motions were compared with both interplate and intraplate real accelerogram records to identify the significance of this effect.

2. MODELLING BUILDING STRUCTURES FOR DYNAMIC ANALYSES

The buildings were modelled as generalised single-degree-of-freedom systems. This form of modelling has been successfully used in previous research and provides a reasonable approximation to the response behaviour of single-storey and multi-storey buildings which satisfy the following conditions:[18,21,22]

(i) The elastic response is dominated by the fundamental mode of vibration.
(ii) The deflected shape does not change significantly after initial yielding [refer Figures 1(a) and 1(b)].

It is imperative that the building be free of structural irregularities such as soft stories or sudden changes in stiffness as shown in Figures 1(c) and 1(d).

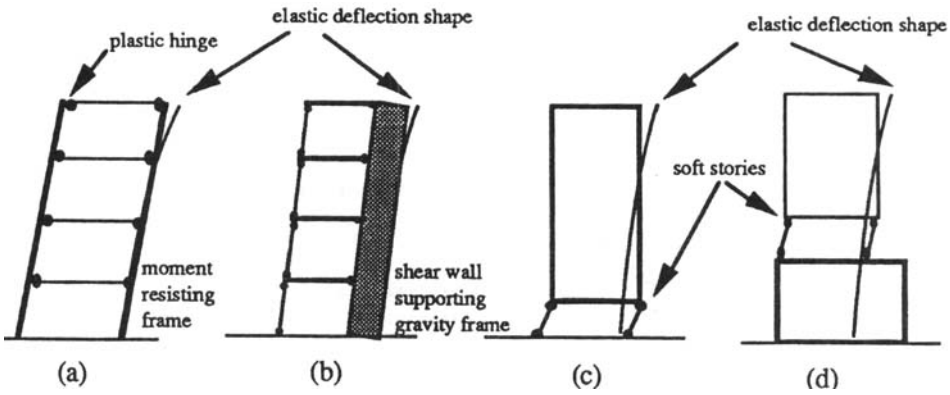

Figure 1. Elastic and inelastic deflected shape of multi-storey frames

The load–displacement relationship of the models assumes elasto-perfectly plastic (EPP) behaviour which neglects stiffness and strength degradation in the model. It has been established that EPP modelling provides reasonably accurate estimates of the inelastic response of a building provided that there is no significant strength degradation. Further, studies have shown that the inelastic hysteretic shape of the load deflection curve does not significantly affect the overall inelastic structural response.[18,19]

Mahin and Bertero[18] concluded in their paper that: 'Stiffness deterioration and moderate amounts of deformation hardening generally appear to have small effects on ductility demands of SDOF systems'.

Moss *et al.*[19] remarked in the discussion section of their paper that: 'provided the structure possesses some inherent damping or energy dissipating mechanism, the response of the structure is rather insensitive to the shape of the hysteretic loop'. The paper concluded that: 'As observed by several other researchers the variation in the hysteretic loop shape is not a major influence in the dynamic response of inelastic structures subjected to earthquake excitation'.

The kinematic ductility demand ratio adopted in this study is defined as the maximum displacement at the top of the building divided by the corresponding displacement at yield. This ductility ratio is a reasonable measure of the overall damage to regular and symmetrical buildings in which the deflected shape is not significantly modified through yielding. It should be noted that this kinematic ductility demand is much less than the curvature and rotational ductility demands experienced locally at a plastic hinge in the structure. Ductility has also been defined in terms of dissipated hysteretic energy which takes into account the contribution of the cyclic loading history.[18]

In most current codes of practice around the world, the seismic base shear resistance F_d of a building is scaled down from the elastic base shear F_e by a load reduction factor R which takes into account overstrength and ductility in the building. As shown in Figure 2, the base shear would normally exceed F_d by a small margin before the first plastic hinge is formed (at F_i). Resistance is further increased as more plastic hinges are developed until the ultimate condition is reached when the resistance starts to deteriorate. This behaviour assumes that the plastic hinges have sufficient rotational ductility to allow these overall deflections. Based on the idealised EPP behaviour as shown in the figure, the load reduction factor R can be expressed as

$$R = \frac{F_e}{F_d} = \frac{F_e}{F_y} \cdot \frac{F_y}{F_d} = R_\mu \cdot R_{OS} \tag{1}$$

where R_μ and R_{OS} are the ductility and overstrength reduction factors respectively (after Reference 23).

Overstrength in buildings depends on many factors including the margin between the design strength and the actual strength, the oversizing of elements, contributions from non-structural elements and the formation of plastic hinges. The actual overstrength is hard to predict as it also depends on the elastic response characteristics to a future earthquake. In this study, elastic analyses have been carried out using each accelerogram to determine the actual elastic strength demand (F_e). The yield strength for each model has

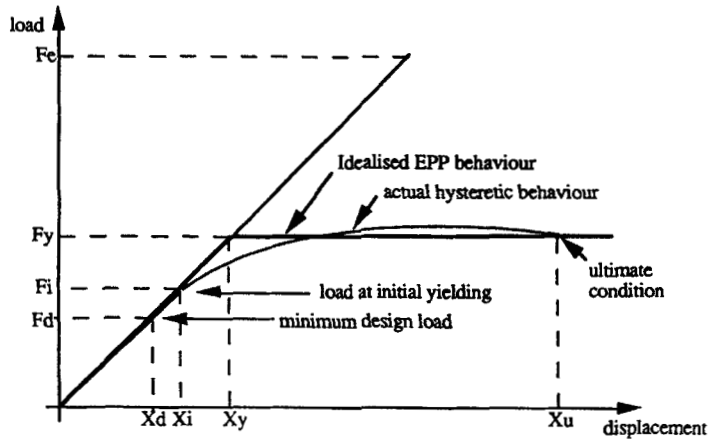

Figure 2. Load versus displacement relationship

been scaled down by $R_\mu = 4$ and R_{OS} has been assumed equal to unity thereby arbitrarily eliminating overstrength. In addition, a separate study (reported later in this paper) was undertaken for other values of R_μ ($R_\mu = 2, 3, 4, 5$ and 6) to correlate directly R_μ with the ductility demand ratio μ, where

$$\mu = \frac{X_u}{X_y} \tag{2}$$

3. GENERATION OF RANDOM PHASE ANGLE SYNTHETIC ACCELEROGRAMS

The acceleration time series $a_g(t)$ generated for synthetic records are based on stationary frequency content as defined by the Fourier amplitude A_n, random phase angles ϕ_n and non-stationary intensity as defined by the time-modulation function $I(t)$[24].

In summary, $a_g(t)$ is defined by the following expression:

$$a_g(t) = I(t) \cdot \sum_{n=1}^{N/2} A_n \sin\left(\frac{2\pi nt}{T} + \phi_n\right) \tag{3a}$$

where $I(t)$ is the exponential function defined by the constants I_0, α and β:

$$I(t) = I_0(e^{-\alpha t} - e^{-\beta t}) \tag{3b}$$

and T is the length of the record and N the number of acceleration time steps with regular intervals Δt (i.e. $N\Delta t = T$).

The α and β constants used in defining the time modulation models have been determined according to the intensity characteristics of a few selected strong motion records.[25] These models were used for generating artificial records with durations of 7, 12 and 26 s (refer Figure 3).

The Fourier amplitude set A_n was determined by an iterative procedure[24] so that the resulting accelerograms matched the target elastic response spectrum defined by one of the following expressions:

$$\text{Sa} = \frac{1{\cdot}25S}{T^{0{\cdot}67}}; \quad \text{Sa} \leqslant 2{\cdot}5 \tag{4a}$$

$$\text{Sa} = \frac{\text{Si}}{T^{1{\cdot}1}}; \quad \text{Sa} \leqslant 2{\cdot}7 \tag{4b}$$

where Sa is the elastic spectral value, T the building's natural period, and S and Si the site amplification factors.

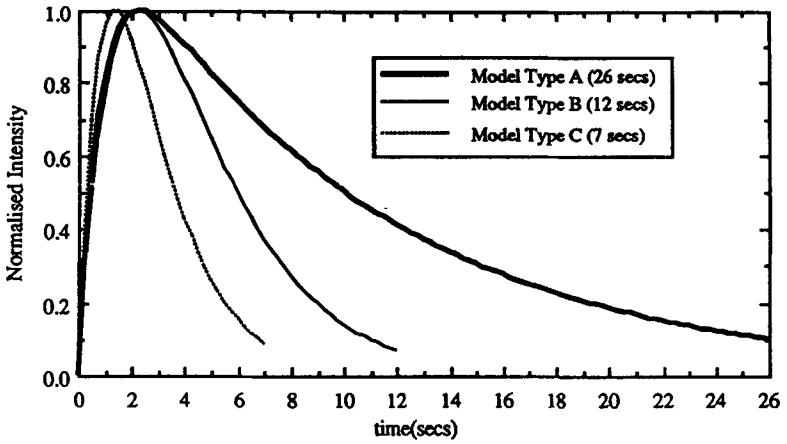

Figure 3. Normalised intensity envelopes of synthetic accelerograms

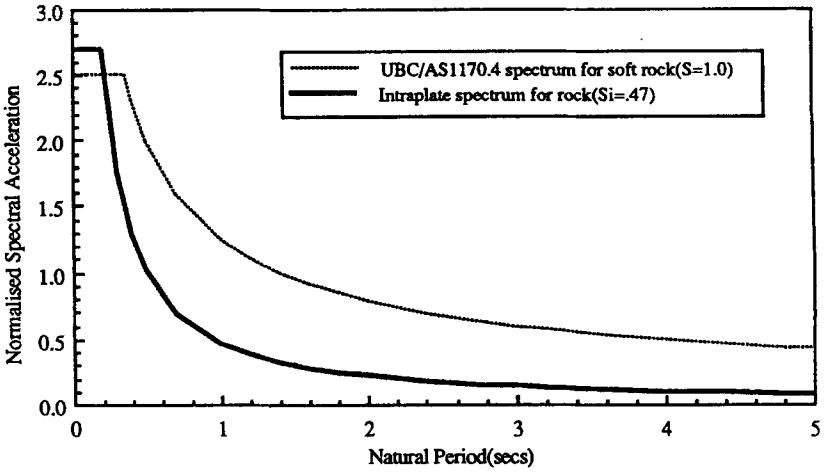

Figure 4. Two of the model target spectra for generation of synthetic accelerograms

The response spectrum defined by equation (4a) for $S = 1{\cdot}0$ based on the Uniform Building Code of the U.S.A.[32] is currently stipulated by the Australian Standard AS1170·4 for soft rock sites[26] and as $S = 0{\cdot}67$ for hard rock sites. The spectrum defined by equation (4b) for $Si = 0{\cdot}47$ based on empirical studies by Algermissen and Leyendecker[15] has recently been proposed for rock sites in intraplate area[13] (refer figure 4). Synthetic records generated for different time intensity functions and target spectra were classified into groups as shown in Table I. A typical artificial accelerogram for a soft rock site ($S = 1{\cdot}0$) with a Type A intensity envelope is shown in Figure 5. Accelerograms for other types of intensity envelopes are similar to Figure 5 except that the intensity of the acceleration trace with time is modulated differently as shown in Figure 3.

4. INTERPRETATION OF RESULTS FROM INELASTIC TIME-HISTORY ANALYSES

The ductility demand obtained from the inelastic analyses based on a load reduction factor $R = 4$ of the synthetic and real accelerograms is discussed under the following sub-section headings:

(a) Random phase angle effects
(b) Earthquake duration

Table I. Details of the synthetic accelerograms used in the study

Elastic Response Target Spectrum Sa	I(t) Model Type (record length)	Number of time-series generated
UBC/AS1170·4 design response spectrum defined by equation (4a) for rock sites ($S = 1{\cdot}0$)[26]	Model Type A (26 s) Model Type B (12 s)	18 18
UBC/AS1170·4 spectrum defined by equation (4a) ($S = 0{\cdot}67$)	Model Type B (12 s)	18
UBC/AS1170·4 spectrum defined by equation (4a) ($S = 1{\cdot}5$)	Model Type A (26 s)	18
UBC/AS1170·4 spectrum defined by equation (4a) ($S = 2{\cdot}0$)	Model Type A (26 s)	18
Model spectrum defined by equation (4b) (Si = 0·47) proposed for intraplate rock sites[13,15]	Model Type B (12 s) Model Type C (7 s)	18 18
Model spectrum defined by equation (4b) (Si = 0·67)	Model Type B (12 s)	18
Model spectrum defined by equation (4b) (Si = 1·0)	Model Type B (12 s)	18
Model spectrum defined by equation (4b) (Si = 1·35)	Model Type B (12 s)	18

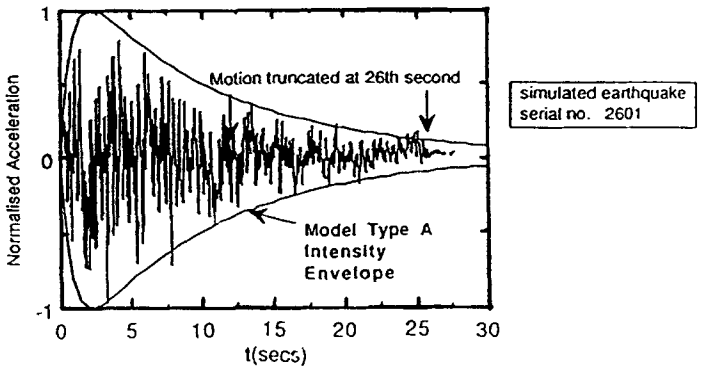

Figure 5. Acceleration-time plot of a synthetic record for rock sites

(c) Earthquake frequency content
(d) Synthetic versus real accelerograms
(e) Regional differences
(f) Kinematic ductility demand ratio versus ductility reduction factor

4.1. Random phase angle effects

Figure 6 presents the kinematic ductility demand obtained from the analyses of 18 synthetic accelerograms whose elastic response spectra are compatible to the model spectrum defined by equation (4b) for Si = 0·47 which has been proposed for use in an intraplate area.[13] Although the frequency content and duration of the individual records are similar, the random variation in the phase angles has caused significant differences in the ductility demand. The random effects can be removed by using the Student t distribution to obtain the 'population average', as shown in Figure 7 and outlined in Appendix I.

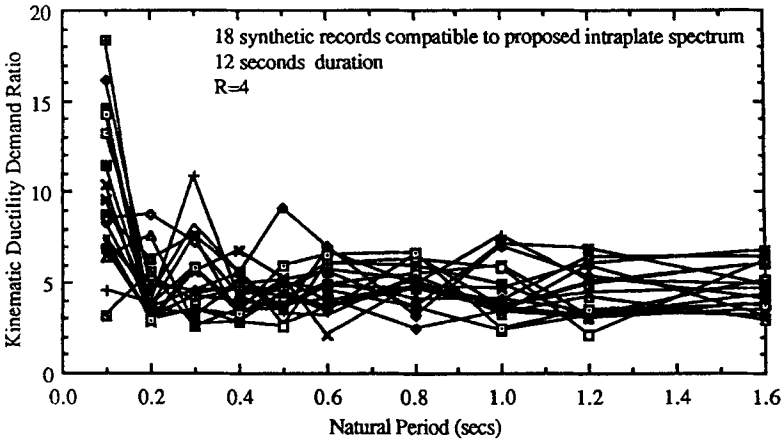

Figure 6. Kinematic ductility demand from 18 synthetic accelerograms

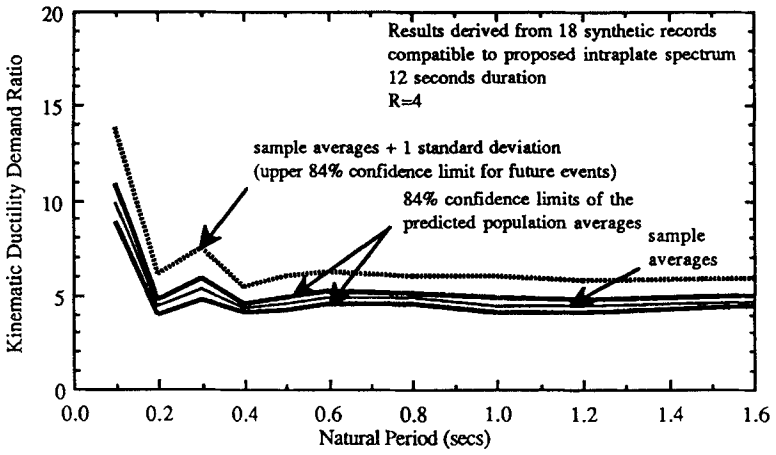

Figure 7. Statistics of results from analyses of the 18 synthetic accelerograms

4.2. Earthquake duration

Eighteen synthetic records (Si = 0·47) each of 7 s and 12 s duration were generated to study the relationship between ductility demand and earthquake duration. The kinematic ductility demand ratio appears to be insensitive to changes in the ground motion duration [Figure 8(a)]. In contrast, the duration significantly affects hysteretic ductility demand which by definition is based on the accumulated dissipated energy caused by cyclic loading. Further, the duration has only a very moderate effect on damage levels predicted by Park and Ang's damage index model [Figure 8(b)].[21] These observations, however, are only valid if the structure responds without significant strength degradation (as is the case in this study using an EPP model). Further, it has been found experimentally and by field observation that ground shaking duration contributes significantly to the actual level of damage sustained.[27]

4.3. Earthquake frequency content

In addition to the 36 synthetic records described above, a further 144 records have been generated in a similar manner with frequency content compatible to different response spectra defined in Table I for a range of soil conditions. Figure 9(a) shows the average elastic spectral acceleration (based on 5 per cent damping) defining the frequency content for each group of synthetic records and Figure 9(b) shows their

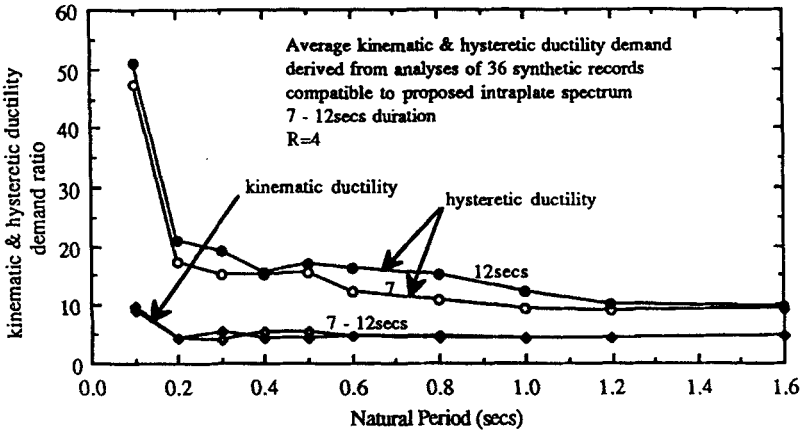

Figure 8(a). Effects of duration on ductility demand ratio

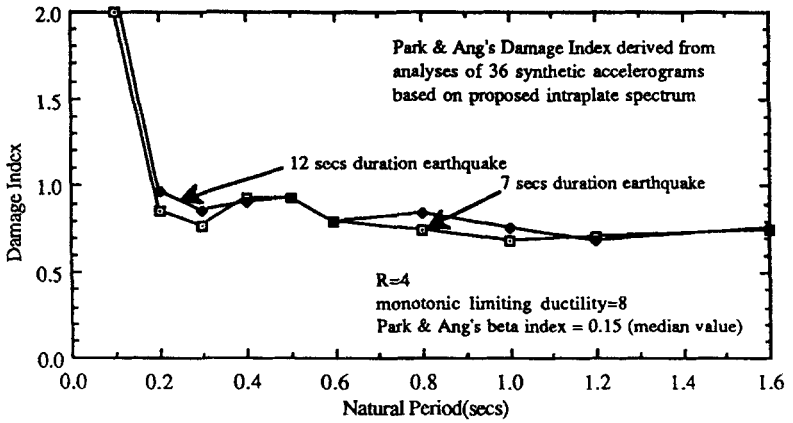

Figure 8(b). Effects of duration on Park and Ang's Damage Index[21]

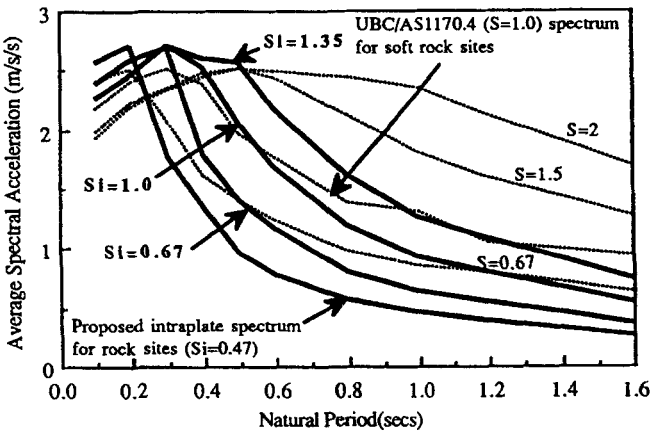

Figure 9(a). Average elastic response spectra of synthetic accelerograms. (·····) Average Spectra of synthetic records based on UBC/AS1170.4 design spectra (Eq. 4a), (——) Average Spectra of synthetic records based on empirically derived model spectra (Eq. 4b)

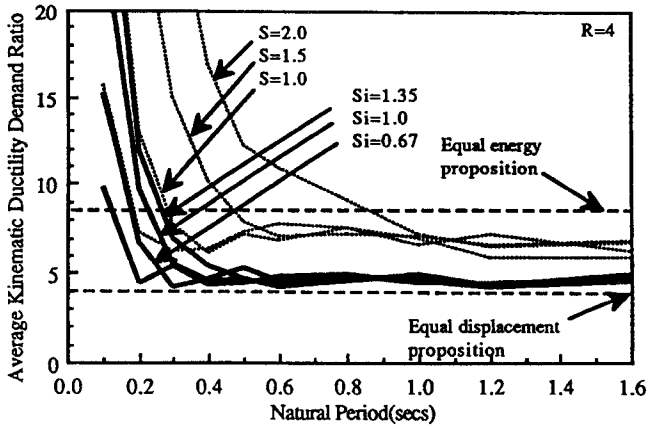

Figure 9(b). Average kinematic ductility demand of synthetic accelerograms. (·····) Average results from synthetic records based on UBC/AS1170.4 design spectra (Eq. 4a), (——) Average results from synthetic records based on empirically derived model spectra (Eq. 4b)

average kinematic ductility demand ratios. Whilst, the ductility demand ratios derived from the compatible response spectra of AS1170·4 [defined by equation (4a)] are in the order of 50 per cent higher than that predicted by the equal displacement definition in the long period range, results from the intraplate spectrum of Reference 13 and other similar spectra [defined by equation (4b)] are generally close to the equal displacement predictions. However, very high ductility demand due to inelastic amplification could occur in buildings with short natural periods depending on the frequency content of the earthquake ground motion. For a short period structure the kinematic ductility demand ratio is much greater in soft soils (which have a greater proportion of low frequency components) than for rock (which have a greater proportion of high frequency components). Clearly, soft soils amplify both the elastic response and inelastic ductility demand of low rise buildings (short period range). Further, the range of natural periods affected by the inelastic site amplifications are dependent on the elastic spectral shape. Currently, most earthquake loading standards account for the elastic amplification but ignore these inelastic amplification effects.

4.4. Synthetic versus real accelerograms

Synthetic accelerograms compatible with response spectra defined by equations (4a) and (4b) (refer Table I and Figure 4) were used to calculate the kinematic ductility demand ratios for a range of buildings with different natural periods. Kinematic ductility demand ratios from the synthetic records were then compared with the results calculated from real accelerograms.

Eighty one of the 105 real accelerograms used in this study were divided into three groups of 29, 24 and 28 records with elastic spectra similar to the model spectra (i.e. similar frequency content) defined by equation (4b) for Si = 0·47, 1·0 and 1·35 [refer Figure 10(a)]. The group of 29 'intraplate' accelerograms (with frequency contents compatible to Si = 0·47) were all recorded within 60 km of the epicentre of earthquakes with a magnitude of at least 5·3. The group consisted of 14 intraplate earthquake records and 15 interplate records which contained a higher than average frequency content. The intraplate accelerograms included two Canadian earthquakes recorded within 50 km of the epicentre: at Nahanni in 1985 (Richter magnitude $M_L = 6{\cdot}9$)[28] and at Saguenay in 1988 ($M_L = 6$).[5] The occurrence of foreshocks provided the rare opportunity to install recording instruments close to the source of these major Canadian events. In addition to the Canadian records, 4 synthetic accelerograms have also been derived from real aftershock records to represent the 1989 Newcastle earthquake ($M_L = 5{\cdot}6$) in Australia.[29] Further details of the records in the ensemble are described in Appendix II.

The average kinematic ductility demand ratios obtained from the random phase angle synthetic accelerograms derived from the model spectra [defined by equation (4b)] were generally consistent with those obtained from the real accelerogram records [refer Figure 10(b)]. In comparison, results derived from the

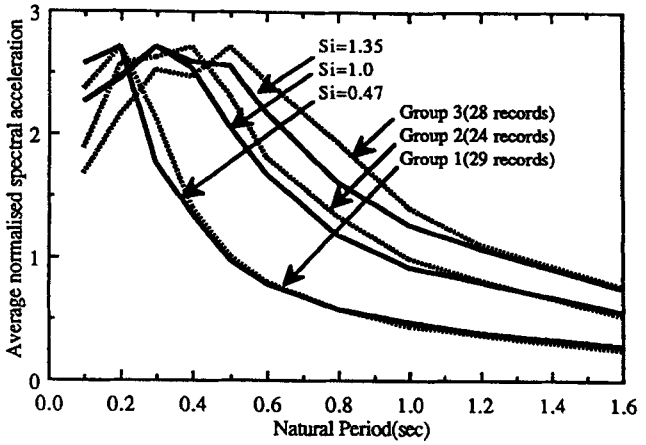

Figure 10(a). Comparison of elastic response spectra from real and synthetic accelerograms. (——) Average Spectra of synthetic records based on empirically derived model spectra (Eq. 4b), (·····) Average Spectra of 81 selected real earthquake records (classified into 3 groups)

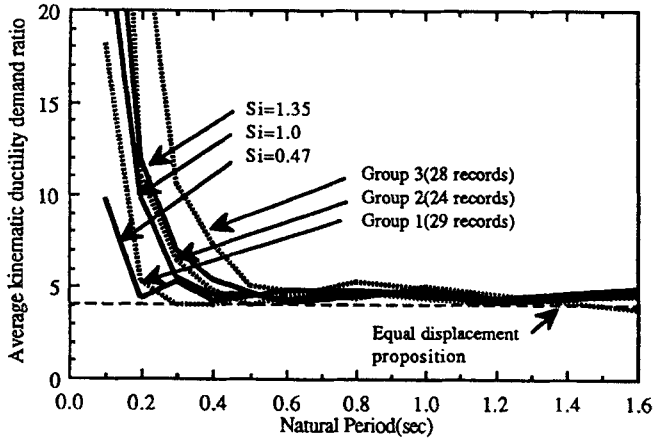

Figure 10(b). Comparison of average kinematic ductility demand from real and synthetic accelerograms. (——) Average results from synthetic records based on empirically derived model spectra (Eq. 4b), (·····) Average results from 81 selected real earthquake records (classified into 3 groups)

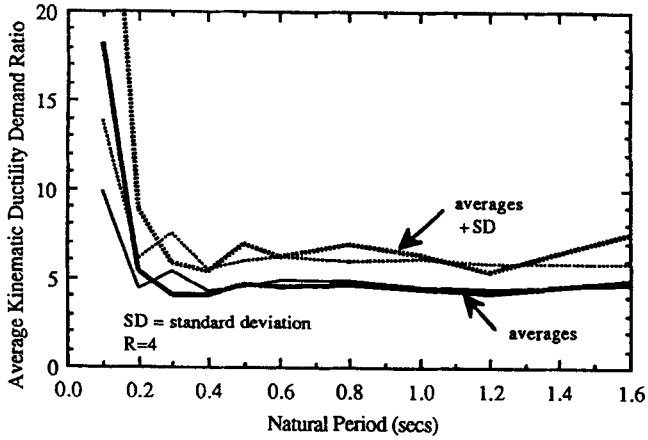

Figure 10(c). Comparison of standard deviation of results from real and synthetic accelerograms. (——) Average results from 18 "intraplate" (Si = 0·47) synthetic records, (·····) Averages + SD, (▬▬) Average results from 29 real records (Group 1), (·····) Averages + SD

AS1170·4 design spectra [defined by equation (4a)] are less representative of real earthquake conditions due to conservatism of the elastic spectra in the long period range [refer Figures 9(a) and 9(b)].

Both the synthetic and real accelerograms consistently showed a high ductility demand for short period buildings which was correlated with the elastic spectral properties (frequency content). However, synthetic records tend to produce less inelastic amplification effects than the real records. The average ductility demand for longer period buildings was approximately equal to the equal displacement prediction ($R = \mu = 4$) and was much less sensitive to changes in the frequency content for both sets of records. The standard deviation of the kinematic ductility demand ratio for buildings subject to both real and synthetic earthquakes with natural periods greater than 0.2 seconds compatible with Si = 0·47 was in the order of 1 to 2 (Figure 10c).

4.5. Regional differences

The influence on the ductility demand characteristics of earthquakes with similar elastic spectral properties but from different regions around the world is studied in this subsection. The group of 29 'intraplate' compatible accelerograms previously described were sorted into subsets according to their location, namely California, the West Pacific, Saguenay, Nahanni, Newcastle and Eastern Europe. Records from the 1994 Northridge earthquake in California have been grouped separately due to their unusual thrust fault source mechanism which is different from the strike slip mechanism typical of most Californian earthquakes. The Saguenay records are also distinguished from other Canadian intraplate records due to a number of observed anomalies.[5] Records from Nahanni have been further divided into two subsets each representing different ranges of the earthquake magnitude.

Although the frequency content of the selected records is similar as reflected in the elastic spectral shape [Figure 11(a)], the phase angles vary considerably. The average kinematic ductility demand ratio for each subset has been determined for the interplate records [Figure 11(b)] and the intraplate records [Figure 11(c)]. The following observations can be made from Figures 11(a)–(c).

A comparison of Figures 11(b) and 11(c) (interplate versus intraplate events) suggests that the kinematic ductility demand ratios are similar for both. It should be noted that this comparison relates to real earthquake records of similar frequency content as distinct from the earlier comparison [Figure 9(b) and 10(b)] made using synthetic records of earthquakes with distinctly different frequency content.

Earthquake ground motions recorded on the same site for events with similar epicentral distances but different magnitudes (e.g. an aftershock) can have significantly different kinematic ductility demand ratios. The average ductility demand for the Nahanni earthquake for shocks of magnitude greater than 6 was

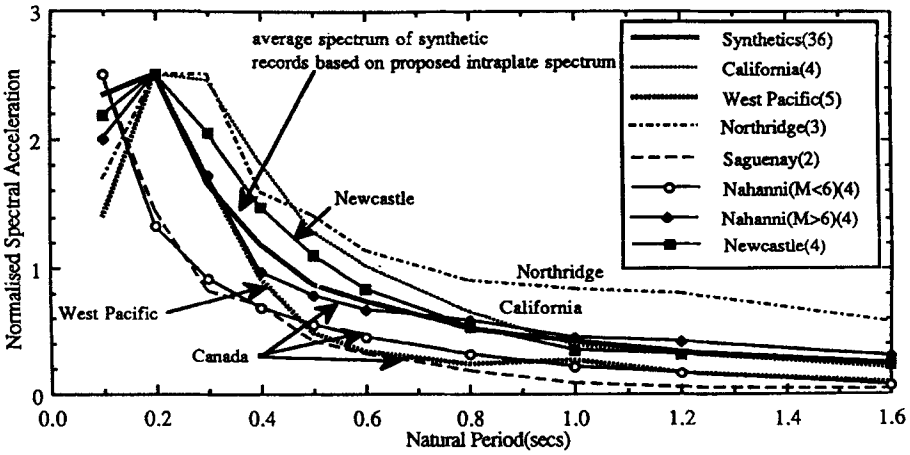

Figure 11(a). Elastic spectral acceleration of selected recorded accelerograms. Figures in ( ) in the legends are the no. of records analysed for each subset

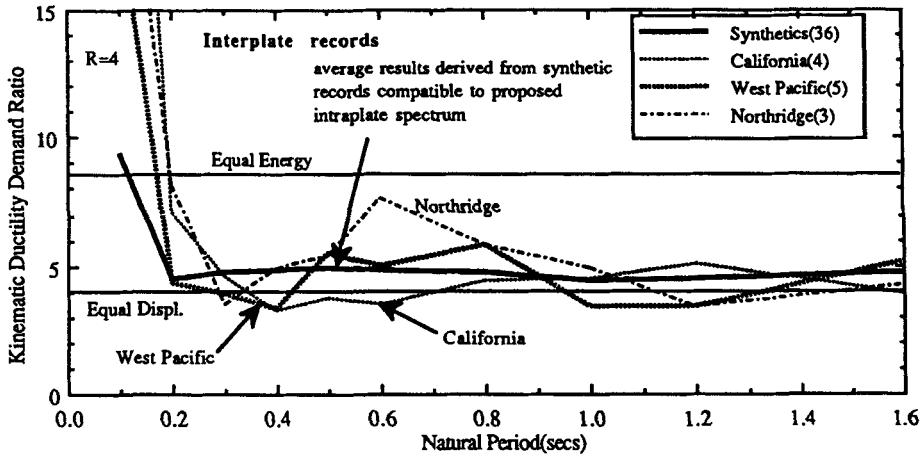

Figure 11(b). Kinematic ductility demand ratio of selected recorded interplate accelerograms. Figures in ( ) in the legends are the no. of records analysed for each subset

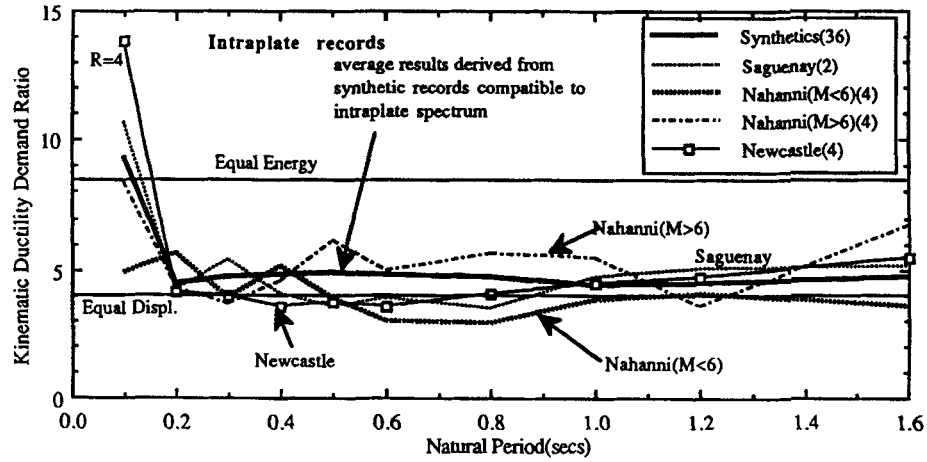

Figure 11(c). Kinematic ductility demand ratio of selected recorded intraplate accelerograms. Figures in ( ) in the legends are the no. of records analysed for each subset

significantly higher than for shocks of magnitude less than 6 [Figure 11(c)]. Similarly, previous Californian earthquake records would not have predicted the exceptionally high ductility demand associated with the Northridge earthquake for buildings with natural periods in the range 0.5–1.0 s [Figure 11(b)].

The El Centro earthquake record (measured during the 1940 Imperial Valley earthquake in southern California) has often been used for benchmarking the seismic response behaviour of buildings. It has been shown, however, that this record has a considerably lower ductility demand than the average ductility demand derived from other earthquake records of similar frequency content for buildings in the low period range. Figure 12(a) presents the normalised elastic response spectrum for the El Centro record together with the average spectra for an ensemble of real records compatible with the UBC/AS1170·4 $S = 1{\cdot}0$ spectrum and the proposed intraplate spectrum. Interestingly, the kinematic ductility demand for the El Centro record was more consistent with the intraplate compatible records (which possess a higher frequency content) than the UBC/AS1170·4 $S = 1{\cdot}0$ records in the low period range.

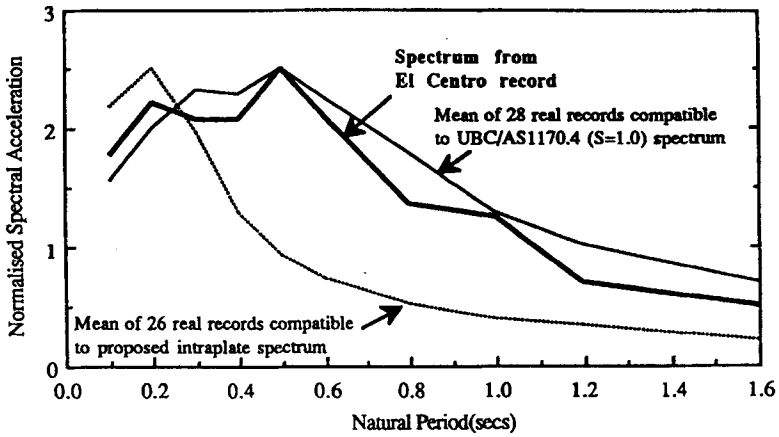

Figure 12(a). Elastic spectral acceleration of El Centro record in comparison with real record ensembles

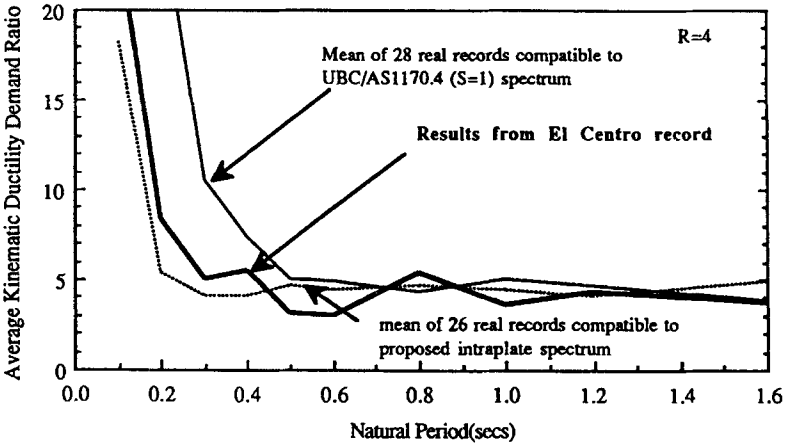

Figure 12(b). Kinematic ductility demand derived from El Centro record in comparison with real record ensembles

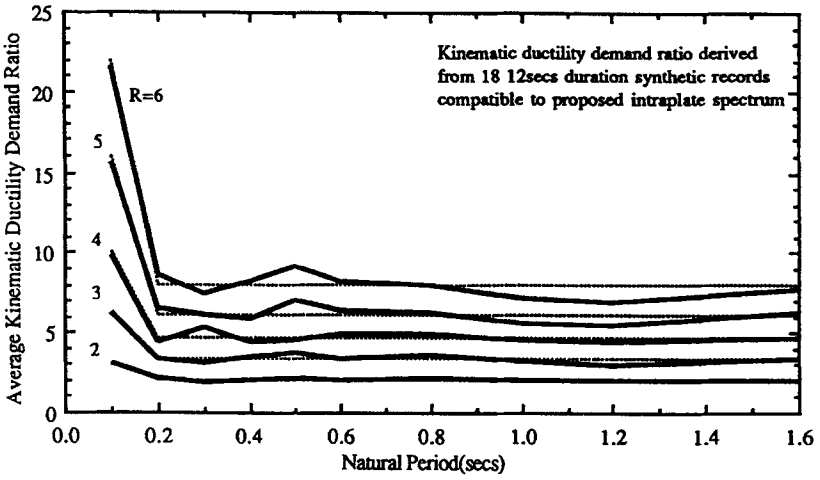

Figure 13(a). Kinematic ductility demand for different R_μ and different building natural periods

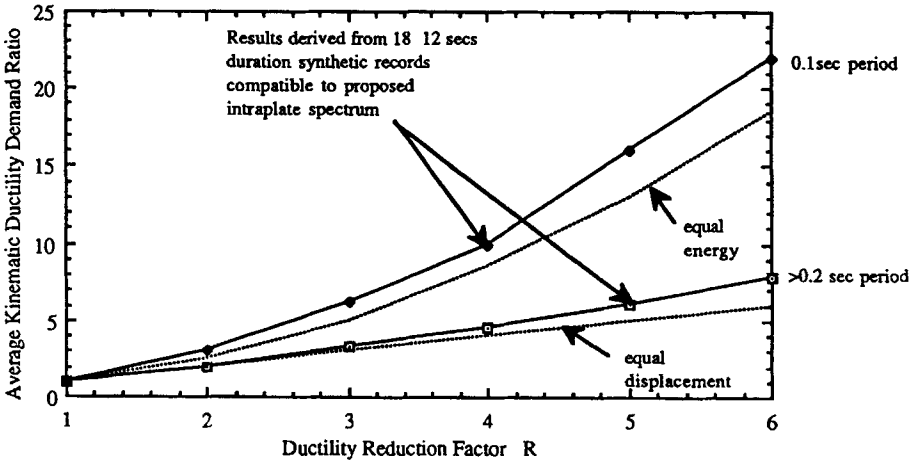

Figure 13(b). Kinematic ductility demand versus ductility reduction factor R_μ

4.6. Kinematic ductility demand ratio versus ductility demand reduction factor

In this section, the relationship between the kinematic ductility demand ratio and the ductility reduction factor ($R_\mu = 2, 3, 4, 5$ and 6) is examined using eighteen 12 s duration synthetic ground motion records compatible with the proposed intraplate model response spectrum for rock.[13] The results are summarised in Figures 13(a) and 13(b) which indicate that the equal displacement definition is valid and recommended for buildings with periods greater than 0·2 s (i.e. most buildings greater than two storeys). For periods less than 0·2 s, the equal energy definition appears to be a better predictor of inelastic response. Whilst these results are meaningful for the target response spectrum considered, extending the analyses to other model spectra has not been considered here. However, the trend for other model spectra can be established from Figure 9(b) for $R_\mu = 4$.

5. CONCLUSIONS

The following conclusions may be drawn:

(i) The equal displacement definition is a good predictor of the *average* kinematic ductility demand for buildings with natural periods greater than the predominant frequency of the ground motion. For ground motions compatible to the proposed intraplate rock spectrum, this corresponds to buildings with natural periods greater than approximately 0·2 s.

(ii) Inelastic amplification effects can cause very high *average* ductility demands for buildings with natural periods less than the predominant frequency of ground motion. The inelastic amplification effect extends from low rise buildings subjected to the model intraplate rock spectrum to both low and medium rise buildings sited on soft soils. Current building standards account for the elastic amplification but ignore these inelastic amplification effects.

(iii) The inelastic response of buildings when subjected to individual earthquake records (associated with the same seismic environment and with similar frequency content and duration) displayed some variation from the overall *average* kinematic ductility demand for the ensemble of records. This is attributed to the variation in phase angles which govern the arrival time and sequence of individual acceleration pulses. For example, the El Centro earthquake produces a considerably lower kinematic ductility demand ratio than the average ductility demand derived from other earthquakes with similar frequency content, for buildings in the low period range.

(iv) The earthquake duration has a much more pronounced effect on the hysteretic ductility demand than both the kinematic ductility demand and Park and Ang's damage index. This observation is based on

an elastic perfectly plastic model without strength degradation. However, it is appreciated that buildings with inadequate detailing may experience strength degradation in which case duration could have a more significant effect.

(v) Synthetic accelerograms derived using random phase angles are generally representative of real earthquake ground motions for inelastic response studies (except for very short period buildings) provided that their elastic spectral properties are compatible. However, results from synthetic records derived for the idealised code design spectra (such as Uniform Building Code and Australian Standard AS1170·4) indicate a significantly higher average ductility demand in the long period range.

(vi) There was little evidence to suggest any inherent differences in the inelastic response behaviour of buildings from intraplate and interplate earthquakes which possessed similar frequency content.

ACKNOWLEDGEMENTS

The authors gratefully acknowledge Gary Gibson and Vaughan Wesson of the Australian Seismology Research Centre, RMIT, Melbourne for their invaluable advice on the seismological aspects of this study and the provision of strong ground motion data. The following persons are also acknowledged for supplying strong motion records: Professor Arthur Heidebrecht (McMaster University, Canada), Dr. Adrian Chandler (University College, London) and Dr Helen Goldsworthy (The University of Melbourne). The work reported in the paper forms part of a joint project between the authors and Gary Gibson and Vaughan Wesson, funded by the Australian Research Council, titled: 'Earthquake Ground Motions and Structural Ductility Factors for Australian Conditions' (Large Grant no. AB9330945).

APPENDIX I. POPULATION AVERAGES AND CONFIDENCE LIMITS OF RESULTS DERIVED FROM ARTIFICIALLY GENERATED RECORDS

Any bias in the results caused by an insufficient number of real accelerograms in an intraplate area is eliminated by the use of a large number of artificially generated earthquake records. The 84 per cent confidence limits of an unbiased average can be obtained from the Student t-distribution model[31] expressed as:

$$\mu_S\left(1-\frac{t_{\alpha=0\cdot16}}{\sqrt{n}}\,\mathrm{cov}\right)\leqslant\mu_p\leqslant\mu_S\left(1+\frac{t_{\alpha=0\cdot16}}{\sqrt{n}}\,\mathrm{cov}\right) \tag{A1}$$

where μ_p is the predicted population average of the ductility demand ratio, μ_S the sample average, cov the sample coefficient of variation, n the number of samples and $t_{\alpha=0\cdot16}$ is the variable for 84 per cent confidence.

A total of 18 synthetic accelerograms with compatible frequency content have been analysed. For $n = 18$ and $t_{\alpha=0\cdot16} = 1\cdot05$, equation (A1) becomes:

$$\mu_S(1-0\cdot25\,\mathrm{cov})\leqslant\mu_p\leqslant\mu_S(1+0\cdot25\,\mathrm{cov}) \tag{A2}$$

Because of the large number of records in the sample, a very narrow confidence limit band has been achieved in the estimate of the population average(refer Figure 7). Thus, the risk of using a biased sample is very small and hence the confidence limit associated with estimating the ductility demand for a future event has improved significantly.

APPENDIX II

Details of 29 strong motion accelerograms with frequency content compatible to proposed intraplate spectrum (defined by equation (4b) for Si = 0·47)

Filename	Event magnitude (note 1)	Epicentral distance (km)	Soil type (note 2)	Max. accel. (m/sec/sec)	Record length (sec)	Details of earthquakes and recording stations
Australia						
syn9·dat	5·6	12	Rock	1·86	20·48	Synthetic records derived from recordings of magnitude 3 aftershock of Newcastle earthquake on 23 Feb., 1990.
syn10.dat	5·6	13	Rock	1·82	20·48	Synthetic records derived from recordings of magnitude 3 aftershock of Newcastle earthquake on 23 Feb., 1990.
syn11.dat	5·6	8·5	Rock	2·16	20·48	Synthetic records derived from recordings of magnitude 3 aftershock of Newcastle earthquake on 23 Feb., 1990.
syn12.dat	5·6	8·5	Rock	1·61	20·48	Synthetic records derived from recordings of magnitude 3 aftershock of Newcastle earthquake on 23 Feb., 1990.
California						
stfer1.dat	6	59	Intermediate	1·21	55·02	Recorded at Ferndale (S44W) during NW California earthquake on 8 October, 1951.
stpar2.dat	5·6	5	Stiff	3·96	42·79	Recorded at Chol. Shandon 5 (N05W) during Parkfield earthquake on 28 June, 1966.
stsaj1.dat	5·8	10	Intermediate	1·17	49·57	Recorded at Bank of America building (N31W) during San Jose earthquake on 5 Sep., 1955.
stsaj2.dat	5·8	10	Intermediate	1·25	51·47	Recorded at Bank of America building (N59E) during San Jose earthquake on 5 Sep., 1955.
newhall1.dat	6·6	20	Alluvium	5·72	59·98	Recorded at Newhall LA county fire station (90deg) during Northridge earthquake on 17 Jan., 1994.
smonica1.dat	6·6	23	Alluvium	8·66	59·98	Recorded at Santa Monica City Hall grounds (90deg) during Northridge earthquake on 17 Jan., 1994.
smonica2.dat	6·6	23	Alluvium	3·63	59·98	Recorded at Santa Monica City Hall grounds (360deg) during Northridge earthquake on 17 Jan., 1994.
Canada						
23dc85s1l. dat	6·4(Mb)	7·5	Rock	10·8	20·36	Recorded at Iverson (long.) during mainshock of Nahanni earthquake on 23 Dec., 1985.
23dc85s1l2 .dat	5·5(Mb)	7·5	Rock	2·24	10·80	Recorded at Iverson (long.) during aftershock of Nahanni earthquake on 23 Dec., 1985.
23dc85s1t. dat	6·4(Mb)	7·5	Rock	13·2	20·44	Recorded at Iverson (trans.) during mainshock of Nahanni earthquake on 23 Dec., 1985.
23dc85s1t2 .dat	5·5(Mb)	7·5	Rock	0·87	10·84	Recorded at Iverson (trans.) during aftershock of Nahanni earthquake on 23 Dec., 1985.
23dc85s3l. dat	6·4(Mb)	22·5	Rock	1·90	19·04	Recorded at Battlement Creek (long.) during mainshock of Nahanni earthquake on 23 Dec., 1985.
23dc85s3t. dat	6·4(Mb)	22·5	Rock	1·82	19·12	Recorded at Battlement Creek (trans.) during mainshock of Nahanni earthquake on 23 Dec., 1985.

25dc85s3l. dat	5·7(Mb)	19	Rock	1·03	9·48	Recorded at Battlement Creek (long.) during 2nd Nahanni earthquake on 25 Dec., 1985.
25dc85s3t. dat	5·7(Mb)	19	Rock	0·87	9·48	Recorded at Battlement Creek (trans.) during 2nd Nahanni earthquake on 25 Dec., 1985.
s16t.his	6·0	43	Rock	1·29	33·97	Recorded at Chicoutimi-Nord(S56E) during Saguenay earthquake on 25 Nov., 1988.
s16l.his	6·0	43	Rock	1·04	33·99	Recorded at Chicoutimi-Nord(S34W) during Saguenay earthquake on 25 Nov., 1988.
Europe/Mid East						
stfru1.dat	6·4	52	Rock	1·56	10·14	Recorded at Tolmezzo (EW) in Italy during Friuli earthquake on 6 May, 1976.
stfru2.dat	6·4	52	Rock	0·98	10·11	Recorded at Tolmezzo (NS) in Italy during Friuli earthquake on 6 May, 1976.
sttab1.dat	7·3	64	Soft	7·35	49·88	Recorded at Tabas (Trans) in Iran during Tabas earthquake on 13 Sept., 1978.
West Pacific						
vh05.dat	5·3	35	Stiff	2·49	15·94	Recorded at Atomic Research Institute (NS), Honshu W. coast, Japan during earthquake on 13 June, 1971.
hi03.dat	5·8	33	Stiff	1·43	27·98	Recorded at Kushiro Central Wharf (NS), Honshu E. coast, Japan during earthquake on 11 May, 1972.
stnze2.dat	unknown	unknown	Rock	1·65	29·90	Recorded at Inangahua (S80W) in New Zealand (S. Island) during earthquake on 25th May, 1968.
stpng1.dat	5·3	6	Rock	1·69	17·98	Recorded at Ridge Site (HB) in PNG during Musa earthquake on 16 Sept., 1971.
stpng3.dat	6·3	49	Stiff	1·30	24·62	Recorded at Lae Base (HA) in PNG during Botany earthquake on 25 Sept., 1971

Details of 24 strong motion accelerograms with frequency content compatible to model spectrum (defined by equation (4b) for Si = 1·0)

Australia						
syn2.dat	5·6	12	1·8 Hz A	2·57	20·48	Synthetic records derived from recordings of magnitude 3 aftershock of Newcastle earthquake on 23 Feb., 1990.
syn4.dat	5·6	13	1·8 Hz A	2·00	20·48	Synthetic records derived from recordings of magnitude 3 aftershock of Newcastle earthquake on 23 Feb., 1990.
syn6.dat	5·6	8·5	1·8 Hz A	2·56	20·48	Synthetic records derived from recordings of magnitude 3 aftershock of Newcastle earthquake on 23 Feb., 1990.
syn8.dat	5·6	8·5	1·8 Hz A	1·94	20·48	Synthetic records derived from recordings of magnitude 3 aftershock of Newcastle earthquake on 23 Feb., 1990.
California						
stfer2.dat	6	59	Intermediate	1·18	55·88	Recorded at Ferndale (N46W) during NW California earthquake on 8 October, 1951.
stpar3.dat	5·6	5	Stiff	4·58	44·04	Recorded at Chol. Shandon 5 (N85E) during Parkfield earthquake on 28 June, 1966.
stsaf1.dat	6·6	26	Stiff	1·51	40·44	Recorded at Ventura Boulevard (N79W) during San Fernando earthquake on 9 Feb., 1971.
stsaf2.dat	6·6	41	Stiff	1·27	42·04	Recorded at Figueroa Street (S37W) during San Fernando earthquake on 9 Feb., 1971.

APPENDIX II (*contd.*)

Filename	Event magnitude (note 1)	Epicentral distance (km)	Soil type (note 2)	Max. accel. (m/sec/sec)	Record length (sec)	Details of earthquakes and recording stations
stsaf3.dat	6·6	39	Stiff	1·35	43·80	Recorded at Wilshire Boulevard (N00E) during San Fernando earthquake on 9 Feb.,1971.
pacdown1.dat	6·6	19	Rock	4·26	30·06	Recorded at Pacoima Dam downstream (265deg) during Northridge earthquake on 17 Jan.,1994.
pacdown2.dat	6·6	19	Rock	4·07	30·06	Recorded at Pacoima Dam downstream (175deg) during Northridge earthquake on 17 Jan.,1994.
sylmarff2. dat	6·6	16	Alluvium	8·27	59·98	Recorded at Sylmar County Hospital Parking Lot (360deg) during Northridge earthquake on 17 Jan.,1994.
Central America						
sal8.dat	5·4(Ms)	4·5	Unknown	3·8	11·66	Recorded at Institute of Urban Construction (90deg) during San Salvadore earthquake on 10 Oct.,1986.
sal23.dat	5·4(Ms)	6·5	Unknown	2·14	23·02	Recorded at Hotel Sheraton (0deg) during San Salvadore earthquake on 10 Oct.,1986.
Europe/Mid East						
stgaz1.dat	7·3	14	Intermediate	7·18	13·02	Recorded at Karakyr Point (EW) , Greece during Gazli earthquake on 17 May, 1976.
stgaz2.dat	7·3	14	Intermediate	5·74	13·44	Recorded at Karakyr Point (NS) , Greece during Gazli earthquake on 17 May, 1976.
stspt2.dat	6·8	27	Intermediate	1·69	23·10	Recorded at Gukasyan (Long) during earthquake at Spitak on 7 Dec., 1988.
sttab2.dat	7·3	64	Soft	7·40	49·88	Recorded at Tabas (Long), Iran during earthquake at Tabas on 13 Sept.,1978
stthsa.dat	5·1	18	Intermediate	3·10	20·01	Recorded at City Hotel (Horiz.A), Thessaloniki, Greece duirng earthquake at Thessaloniki on 20 June, 1978.
West Pacific						
stnze3.dat	6·7	117	Stiff	1·15	25·98	Recorded at Massey University (S58W), New Zealand during Central North Island earthquake on 5 Jan., 1973.
stnze4.dat	6·2	51	Stiff	0·84	29·98	Recorded at Vogel Building (N88W) during earthquake near Cook Strait, New Zealand on 18 Jan., 1977.
hi15.dat	7·4	116	Rock	2·23	57·94	Recorded at Ofunato Harbour Works, Japan during earthquake near East Coast of Honshu on 12 June, 1978.
in05.dat	7·0	196	Stiff	0·76	59·90	Recorded at Kushiro Central Wharf, Japan during earthquake near South Coast of Honshu on 2 Aug., 1971.
lo08.dat	7·9	290	Stiff	2·22	89·86	Recorded at Muroran Harbour, Japan during earthquake near East Coast of Honshu on 16 May, 1968.
Details of 28 strong motion accelerograms with frequency content compatible to model spectrum (defined by equation (4b) for Si = 1·35)						
Australia						
syn1.dat	5·6	12	Alluvium	2·18	20·48	Synthetic records derived from recordings of magnitude 3 aftershock of Newcastle earthquake on 23 Feb., 1990.

syn3.dat	5·6	13	Alluvium	1·68	20·48	Synthetic records derived from recordings of magnitude 3 aftershock of Newcastle earthquake on 23 Feb., 1990.
syn5.dat	5·6	8·5	Alluvium	2·30	20·48	Synthetic records derived from recordings of magnitude 3 aftershock of Newcastle earthquake on 23 Feb., 1990.
syn7.dat	5·6	8·5	Alluvium	1·94	20·48	Synthetic records derived from recordings of magnitude 3 aftershock of Newcastle earthquake on 23 Feb., 1990.
California						
stelc1.dat	6·6	8	Stiff	3·06	29·16	Recorded at El Centro (NS) during Imperial Valley earthquake on 18 May, 1940.
stker1.dat	7·6	120	Soft	0·43	59·92	Recorded at Hollywood (EW) during Kern County earthquake on 21 July, 1952.
stker2.dat	7·6	120	Soft	0·61	59·74	Recorded at Hollywood (NS) during Kern County earthquake on 21 July, 1952.
stpar1.dat	5·6	7	Soft	4·98	43·78	Recorded at array no.2 station (N65E) during Parkfield earthquake on 28 June, 1966.
stpre1.dat	7·1	105	Intermediate	2·01	14·12	Recorded at Presidio (90deg) during Loma Prieta earthquake on 17 Oct., 1989.
stpre2.dat	7·1	105	Intermediate	0·96	14·20	Recorded at Presidio (0deg) during Loma Prieta earthquake on 17 Oct., 1989.
arleta1.dat	6·6	10	Alluvium	3·37	59·98	Recorded at Arleta fire station (90deg) during Northridge earthquake on 17 Jan., 1994.
arleta2.dat	6·6	10	Alluvium	3·02	59·98	Recorded at Arleta fire station (360deg) during Northridge earthquake on 17 Jan., 1994.
newhall2·dat	6·6	20	Alluvium	5·78	59·98	Recorded at Newhall LA County fire station (360deg) during Northridge earthquake on 17 Jan., 1994.
sylmarff1. dat	6·6	16	Alluvium	5·93	59·98	Recorded at Sylmar County Hospital (Parking Lot) (90deg) during Northridge earthquake on 17 Jan., 1994.
Canada						
23dc85s2l. dat	6·4(Mb)	7·5	Rock	3·83	18·76	Recorded at Slide Mountain (long.) during mainshock of Nahanni earthquake on 23 Dec., 1985.
23dc85s2t. dat	6·4(Mb)	7·5	Rock	5·35	18·80	Recorded at Slide Mountain (trans.) during mainshock of Nahanni earthquake on 23 Dec., 1985.
Europe/Mid East						
stleu1.dat	5·7	Unknown	Intermediate	4·09	23·15	Recorded at Leukas (Long.) in Greece during Leukas earthquake on 4 Nov., 1973.
Central America						
sal2.dat	5·4(Ms)	5·5	Unknown	5·24	20·0	Recorded at National Geograhical Inst. (70deg) during San Salvadore earthquake on 10 Oct., 1988.
sat2.dat	5·4(Ms)	5·5	Unknown	3·92	20·3	Recorded at National Geograhical Inst. (180deg) during San Salvadore earthquake on 10 Oct., 1988.
sal5.dat	5·4(Ms)	4·0	Unknown	4·12	9·10	Recorded at Geotechnical Investigation Centre (180deg) during San Salvadore earthquake on 10 Oct., 1988.
sat5.dat	5·4(Ms)	4·0	Unknown	6·81	9·10	Recorded at Geotechnical Investigation Centre (270deg) during San Salvadore earthquake on 10 Oct., 1988.

APPENDIX II (*contd.*)

Filename	Event magnitude (note 1)	Epicentral distance (km)	Soil type (note 2)	Max. accel. (m/sec/sec)	Record length (sec)	Details of earthquakes and recording stations
sal11.dat	5·4(Ms)	5·0	Unknown	3·39	21·42	Recorded at Hotel Camino (90deg) during San Salvadore earthquake on 10 Oct., 1988.
sat11.dat	5·4(Ms)	5·0	Unknown	4·21	21·42	Recorded at Hotel Camino (180deg) during San Salvadore earthquake on 10 Oct., 1988.
sal20.dat	5·4(Ms)	4·0	Unknown	3·74	22·7	Recorded at Centro Americana University (180deg) during San Salvadore earthquake on 10 Oct., 1988.
sat20.dat	5·4(Ms)	4·0	Unknown	4·09	22·7	Recorded at Centro Americana University (270deg) during San Salvadore earthquake on 10 Oct., 1988.
West Pacific stnze1.dat	7	33	Intermediate	0.88	29·98	Recorded at Milford Sound Hotel (S41E) in New Zealand during Milford Sound earthquake on 4 May, 1976.
stpng2.dat	7·9	201	Stiff	1·15	59·96	Recorded at Bouganville (HB) in PNG during Panguna earthquake on 14 July, 1971.
lo03.dat	7·4	112	Stiff	2·01	86·92	Recorded at Kushiro Central Wharf (NS), Honshu E. coast, Japan during earthquake on 17 June, 1973.

1. Event magnitude is based on Richter (local) scale unless otherwise indicated. Mb and Ms denotes body wave and surface wave magnitude respectively.
2. Site classification 'rock', 'stiff', 'intermediate' and 'soft' corresponds approx. to Uniform Building Code UBC88 soil types S_1–S_4 respectively.

REFERENCES

1. D. Denham, 'Intraplate earthquakes — why?' in *Proc. Australian earthquake engineering society conference*, Sydney, 3–6, 1992.
2. G. L. Hutchinson, L. Pham and J. L. Wilson, 'Earthquake resistant design of steel structures — an introduction for the practising engineer', *J. Australian institute of steel construction* **28**(2), 6–22 (1994).
3. Institution of Engineers, Australia (ed: Melchers, R.): '*Newcastle Earthquake Study*' (1990).
4. D. M. Boore and G. M. Atkinson, 'Stochastic prediction of ground motion and spectral response parameters at hard rock sites in Eastern and North America', *Bull. seism. soc. Am.* **77**(2), 440–467 (1987).
5. D. M. Boore and G. M. Atkinson, 'Source Spectra For The 1988 Saguenay, Quebec, Earthquakes', *Bull. seism. soc. of Am.* **82**(2), 663–719 (1992).
6. H. Bungum, A. Dahle , G. Toro, R. McGuire and O. T. Gudmestad, 'Ground motions from intraplate earthquakes' in *Tenth world conference on earthquake engineering*, Rotterdam, **2**, 611–616 (1992).
7. A. Dahle, H. Bungum and L. B. Kvamme, 'Attenuation models inferred from intraplate earthquake recordings', *Earthquake eng. struct. dyn.* **19**, 1125–1141 (1990).
8. B. A. Gaull, M. O. Michael-Leiba and J. M. W. Rynn, 'Probabilistics earthquake risk maps of Australia', *Australian j. earth sci.* **37**, 169–187 (1990).
9. N. N. Ambraseys, 'The prediction of earthquake peak ground acceleration in Europe' *Earthquake eng. struct. dyn.* **24**, 467–490 (1995).
10. W. K. Pun and N. N. Ambraseys, 'Earthquake data review and seismic hazard review for the Hong Kong region', *Earthquake eng. struct. dyn.* **21**, 433–443 (1992).
11. Standards Association of Australia, 'Minimum design loads on structures: Part 4: Earthquake Loads — commentary', Supplement to AS1170·4, 1993.
12. G. L. Hutchinson, P. Mendis and J. L. Wilson, 'A review of the new Australian earthquake loading standard, AS1170·4', *Australian civil eng. trans.* **CE36**(3), 235–243 (1994).
13. D. M. Scott, J. W. Pappin and M. K. Y. Kwok, 'Seismic design of buildings in Hong Kong', *Hong Kong institution Eng. trans.* **1**(2), 37–50 (1994).
14. T. C. Hanks and R. K. McGuire, 'The character of high-frequency strong ground motion', *Bull. seism. soc. Am.* **71**(6), 2071–2095 (1981).
15. S. T. Algermissen and E. V. Leyendecker, 'A technique for uniform hazard spectra estimation in the U.S.' in *Proc. 10th world conference on earthquake engineering*, Rotterdam **1**, 391–397 (1992).
16. K. S. P. De Silva, P. A. Mendis, and W. R. Grayson, 'Typical Intra-plate linear design response spectrum', *Australian civil eng. trans.* **CE36**(4), 339–345 (1994).
17. B. Samali, S. Parsanejad and M. Peterson, 'Response Spectra for Australian Earthquake', *Australian civil eng. trans.* **CE36**(1) 89–96 (1994).
18. S. A. Mahin and V. V. Bertero, 'An evaluation of inelastic seismic design spectra', *Journal of Structural Division*, American Society of Civil Engineers **107**(ST9), 1777–1795 (1981).
19. P. J. Moss, A. J. Carr and A. H. Buchanan, 'Seismic response of low-rise buildings', *Bull. New Zealand national soc. earthquake eng.* **19**(3), 180–198 (1986).
20. V. V. Bertero, 'State-of-the-Art Report: Ductility based Structural Design' in *Proc. 9th world conference on earthquake engineering*, Tokyo-Kyoto, Japan, **VIII**, 2–9 (1988).
21. E. Cosenza, G. Manfredi, and R. Ramasco, 'The use of damage functionals in earthquake engineering: a comparison between different methods', *Earthquake eng. struct. dyn.* **22**, 855–868 (1993).
22. E. Miranda, Evaluation of site-dependent inelastic seismic design spectra', *J. struct. eng.* American Society of Civil Engineers **119**(5), 1319–1338 (1993).
23. C. M. Uang, 'Seismic Force Reduction and Displacement Amplification Factors', *J. struct. eng.* **117**(1), 19–28 (1991).
24. Massechussett Institute of Technology, '*SIMQKE: A program for artificial motion generation. Users manual and documentation*' (1976).
25. N. T. K. Lam, '*Assessment of torsion in regular multi-storey buildings subjected to earthquake ground motion*', *Ph.D. Thesis*, The University of Melbourne, 1993.
26. Standards Association of Australia, '*Minimum design loads on structures: Part 4: Earthquake Loads*', AS1170·4, 1993.
27. H. Tiedmann, '*Earthquake and Volcanic Eruptions — A handbook on risk assessment*', Swiss Reinsurance Company, Switzerland (1992).
28. A. C. Heidebrecht and N. Naumoski, 'Engineering implications of the 1985 Nahanni earthquakes', *Earthquake eng. struct. dyn.* **16**, 675–690 (1988).
29. G. Gibson, 'Artificial Ground Motions', *Proceedings of a seminar on Earthquake Engineering and Disaster Reduction*, The University of Melbourne, Melbourne, 83–86 (1993).
30. N. T. K. Lam, J. L. Wilson and G. L. Hutchinson, 'The dependence of ductility demand on the frequency characteristics of earthquake ground motion', *Proc. 14th Australasian conference on the mechanics of structures and materials*, University of Tasmania, Hobart, **1**, 290–295 (1995).
31. J. L. Devore, '*Probability and Statistics for Engineering and the Sciences*', Brooks, Cole and Nelson, Melbourne, 1988.
32. International Conference of Building Officials, U.S.A., '*Uniform Building Code*', Chap. 23, part 3: Earthquake Design (1991).